ISSN 0016-7029, Geochemistry International, 2006, Vol. 44, No. 4, pp. 327–337. © Pleiades Publishing, Inc., 2006.
Original Russian Text © L.K. Levskii, N.M. Stolbov, E.S. Bogomolov, I.M. Vasil'eva, E.M. Makar'eva, 2006, published in Geokhimiya, 2006, No. 4, pp. 365–376.

Sr–Nd–Pb Isotopic Systems in Basalts of the Franz Josef Land Archipelago

L. K. Levskii*, N. M. Stolbov, E. S. Bogomolov*, I. M. Vasil'eva**, and E. M. Makar'eva*****

**Institute of Precambrian Geology and Geochronology, Russian Academy of Sciences, nab. Makarova 2, St. Petersburg, 199034 Russia*

e-mail: geochron@sf13883.spb.edu

***All-Russia Research Institute of Geology and Mineral Resources of the World Ocean, Angliiskii pr. 1, St. Petersburg, 190121 Russia*

****Polar Marine Prospecting Expedition, ul. Pobedy 24, Lomonosov, St. Petersburg, Russia*

Received June 24, 2004

Abstract—Rb, Sr, Sm, Nd, U, and Pb contents and Sr, Nd, and Pb isotopic composition were determined in tholeiite and subalkaline basalts (in both whole-rock samples and individual minerals) from the Franz Josef Land Archipelago. Isotopic data obtained for the Arctic basin are similar to those for islands from the Pacific, Atlantic, and Indian oceans. The assimilation of crustal (sedimentary) rocks by primary depleted material makes isochron determination of basalt age difficult or impossible. The subalkaline basalts (basaltic andesites) were presumably formed by the metasomatic introduction of incompatible elements in tholeiitic basalts and, only partially, through crustal contamination and fractional crystallization.

DOI: 10.1134/S0016702906040021

INTRODUCTION

A great number of isotope–geochemical data are available on islands of the Pacific, Atlantic, and Indian oceans [1–13 and references therein] (mainly in the southern hemisphere), whereas data on island basalts of Arctic basins are practically absent, with the exception only of those recently published in [14, 15]. The pioneering paper [15] reports numerous Sm–Nd and Rb–Sr isotope data on rocks from the Franz Josef Archipelago. Our research of basalts from the Franz Josef Land (FJL) was aimed at deciphering the origin of oceanic basalts from around the world and the significance of FJL in the formation of the continent–ocean transition zone.

Our research was focused on the following problems:

(1) Isotope–geochronological (K–Ar, Rb–Sr, Sm–Nd) investigations of basalts from islands of archipelago (whole-rock and mineral samples);

(2) Position of the FJL rocks in the global Sr–Nd–Pb isotopic systematics;

(3) Influence of crustal component in basalts on equilibrium of the isotopic systems.

GEOLOGICAL SETTING

The Franz Josef Land Archipelago is the separate marginal domal uplift located in the north of the Barents–Kara shelf plate, which borders with the deep-water Nansen depression of the Arctic Ocean. The uplift is bounded by the graben-like superimposed Franz Victoria deep in the west and by the St. Anna trough in the east. Its northern side was uplifted in the Mesozoic–Cenozoic and destructed in the Late Jurassic–Early Cretaceous, with development of trap magmatism in the marginal–shelf uplift of FJL.

The trap complex of the FJL archipelago includes dikes, sills, flows, and vents of volcanic edifices (necks), as well as small subvolcanic stocks. Two volcanoplutonic associations are distinguished among the FJL rocks: low-K tholeiites and subalkaline basaltic andesites [16]. A petrographic study showed their comparatively uniform composition, with the predominance of porphyritic and glomeroporhyritic olivine-free basalts. The amount of olivine in the olivine-bearing tholeiites is insufficient to distinguish them as an independent group. Olivine is commonly replaced by iddingsite–bowlingite, chloropheite, and chlorite. Plagioclase and clinopyroxene occur in several (typically, two–three) generations. The plagioclase composition corresponds to bytownite–labradorite, with a more calcic (up to 75% anorthite) composition of phenocrysts relative to groundmass microliths. The clinopyroxene is typically augite. Orthopyroxene occurs sporadically. All of the rocks of the trap complex contain disseminated opaque minerals, mainly, Ti-magnetite. The basaltic andesites have a glassy groundmass often containing taxitic domains of moderately-acid brown glass. The textures are tholeiitic, poikilophitic, intersertal, and doleritic. The structures range from massive to amygdaloidal. The most fully crystallized rocks in the

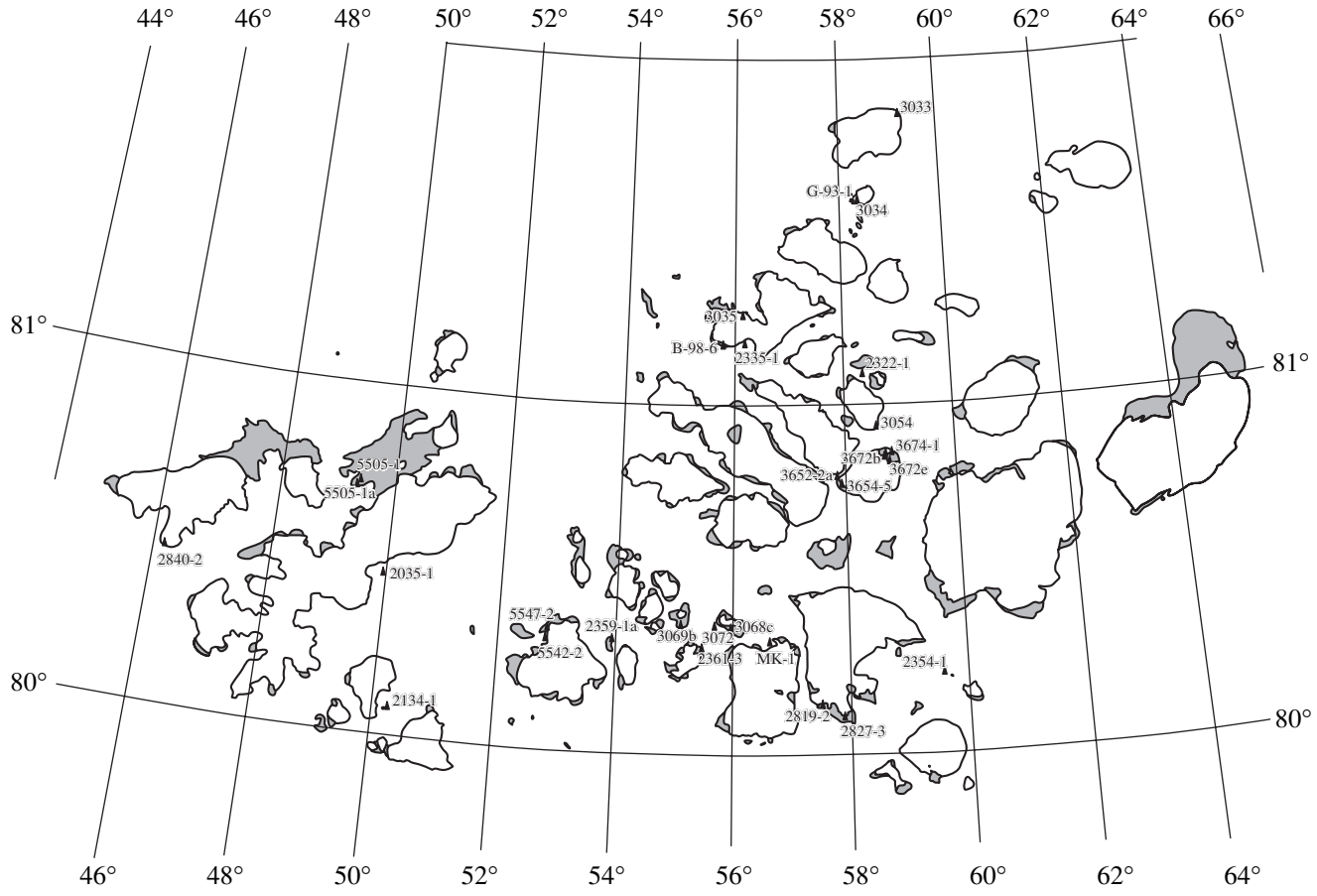

Fig. 1. Map of the Franz Josef Land Archipelago. Triangles denote sampling sites; (2354-1) Albatros (Gokhshteter islands); 2134-1 Windword; (2359-1a) Royal Society; (5542-2 and 5547-2) Guker; (5505-1 and 5505-1a) Georg Land; (2035-1) Nezametnyi; 2819-2 and 2827-3 Gallja; (3069b) Brjus; (3033) Rudolf; (3652-2a, 3654-5, 3672b, 3672e, 3674-1) Wiener Neustadt; (3072) Matilda; (2322) Brosh; (B-98-6 and 3035) Jackson; (3054) Grili; (G-93-1 and 3034) Gegenloe; (2840-2) Aleksandra Land; (2335-1) Kverini; (2361-3) Bredi; (MK-1) Mak Klintok; (3068c) Aldscher.

central part of the flow grade into finer grained varieties toward its top and bottom, while the near-contact rocks contain 90% weakly devitrified glassy mesostasis.

The low-K tholeiites belong to the low-K_2O (<0.4%) sodium series with low contents of SiO_2, TiO_2, total alkalis, P_2O_5, and relatively high contents of Al_2O_3, CaO, and MgO. The subalkali basalts (basaltic andesites) are K–Na rocks and show the opposite proportions of major oxides. Based on ICP-MS data, the subalkali basalts (basaltic andesites) are high in Zn, Ba, Rb, Sr, Zr, Y, REE, and in volatile B and CO_2. By contrast, the tholeiitic basalts are enriched in Cu, Cr, and Ni. Co and V show unsystematic variations [16, 17].

The age of the rocks determined by K–Ar, Ar–Ar, and Sm–Nd methods ranges within 95–161 Ma [18]. Paleontological data suggest that volcanic and, especially, subvolcanic varieties of the subalkali basalts–basaltic andesites were emplaced earlier (Late Tithonian) than the low-K tholeiites (Albian). The simultaneous occurrence of the basalts of both associations in the same exposures can be inferred from the coronary model of a highly advanced front of magma formation.

SELECTION OF SAMPLES AND ANALYTICAL TECHNIQUES

Figure 1 demonstrates a map of FJL and the sampling sites of low-K tholeiite and subalkali basaltic andesites.

Rb–Sr and Sm–Nd isotope analyses were performed by isotope dilution to determine the Rb, Sr, Sm, and Nd contents. The preliminarily grouped samples were spiked with ^{85}Rb-^{84}Sr and ^{149}Sm-^{150}Nd mixed spikes. Then the samples were decomposed in a mixture of HNO_3 and HF. Sr was extracted with cationic chromatography on a AG50W-X8 cation exchanger. Sm and Nd were extracted in two stages. The first stage involved cation-exchange chromatography on a AG50W-X8 cation exchanger with the aim of separating REEs from the rocks and minerals. The second stage involved extraction chromatography with liquid cation-exchange HDEHP supported by Teflon powders.

Table 1. U–Pb isotopic data on rocks and minerals

No.	Sample	Pb (ppm)	U (ppm)	$^{238}U/^{204}Pb$	$^{206}Pb/^{204}Pb$	$^{207}Pb/^{204}Pb$	$^{208}Pb/^{204}Pb$
1	2035-1	3.77	0.950	16.28	19.26 (18.95)	15.61 (15.60)	38.97
2	2035-1*	4.06	0.890	14.17	19.22	15.61	38.92
3	2134-1	2.06	0.345	10.77	18.98 (18.78)	15.59 (15.58)	38.72
4	2134-1*	1.78	0.120	4.28	18.74	15.49	38.29
5	2322-1	1.16	0.232	12.90	18.97 (18.73)	15.59 (15.58)	38.74
6	2322-1*	0.59	0.111	12.04	18.74	15.45	38.38
7	2335-1*	1.18	0.186	10.02	18.91	15.54	38.51
8	2354-1*	2.30	0.497	13.89	19.07	15.58	38.80
9	2359-1a*	3.85	0.833	13.93	19.03	15.58	28.82
10	2361-3*	3.94	0.986	16.13	19.07	15.59	28.87
11	3672·	3.60	0.404	7.21	18.84 (18.70)	15.60 (15.59)	28.81
12	5547/2	1.45	0.267	11.78	18.88 (18.66)	15.59 (15.58)	28.76
13	G-93-1	1.06	0.281	17.10	19.03 (18.71)	15.61 (15.59)	28.84
14	B-98-6	3.74	0.885	15.17	18.95 (18.66)	15.55 (15.54)	28.68
15	5542/2	7.98	1.46	11.81	19.02 (18.76)	15.64 (15.63)	39.13
16	MK-1	1.77	0.446	16.23	19.03 (18.72)	15.59 (15.58)	38.74
17	5505-1	–	–	–	18.93	15.63	38.91
18	3033 whole-rock	0.893	0.228	16.34	18.86 (18.55)	15.57 (15.55)	38.62
19	3033 plagioclas	1.111	0.054	3.17	17.73	15.51	41.32
20	3034 whole-rock	1.04	0.227	13.94	18.95 (18.69)	15.57 (15.56)	38.68
21	3034 plagioclas	0.846	0.051	3.83	18.69	15.57	38.48
22	3035 whole-rock	0.972	0.213	14.02	18.95 (18.69)	15.56 (15.55)	38.66
23	3035 plagioclas	0.569	0.024	2.69	18.58	15.58	38.43

* Samples were preliminarily leached. Numbers in parentheses are isotopic ratios calculated for 120 Ma.

The isotope analysis of Rb, Sr, Sm, and Nd was performed on an eight-collector MAT 261 mass spectrometer in static mode. To correct for isotope fractionation, the Sr isotope ratios were normalized to $^{88}Sr/^{86}Sr = 8.37521$. The normalized values were brought to $^{87}Sr/^{86}Sr = 0.71025$ of the NBS-987 internationally certified isotopic standard. The Nd isotope ratios were normalized to $^{148}Nd/^{144}Nd = 0.241578$ to correct for Nd isotope fractionation. The normalized ratios were brought to the $^{143}Nd/^{144}Nd = 0.511860$ in the La Jolla international standard. The Rb, Sr, Sm, and Nd contents were measured accurately to 0.5%. The laboratory blanks were 30 pg for Rb, 30 pg for Sr, 30 pg for Sm, and 70 pg for Nd.

Replicate analyses of the BCR-1 international standard gave the following values: Rb = 45.9 μg/g, Sr = 329 μg/g, $^{87}Rb/^{86}Sr = 0.4027 \pm 9$, $^{87}Sr/^{86}Sr = 0.705013 \pm 6$ (average of six determinations); Sm = 6.45 μg/g, Nd = 28.4 μg/g, $^{147}Sm/^{144}Nd = 0.1383 \pm 3$, $^{143}Nd/^{144}Nd = 0.512654 \pm 8$ (average of ten determinations). The construction of the isochrons and the calculation of age, initial $(^{87}Sr/^{86}Sr)_0$ and ε_{Nd} values, were conducted with an ISOPLOT program, using the following decay constants: $\lambda_{^{87}Rb} = 1.42 \times 10^{-11}$ yr^{-1}, $\lambda_{^{147}Sm} = 6.54 \times 10^{-12}$ yr^{-1}, $(^{143}Nd/^{144}Nd_{CHUR})_0 = 0.512636$, $(^{147}Sm/^{144}Nd_{CHUR})_0 = 0.1967$. The following values of analytical errors were input during the Rb–Sr and Sm–Nd calculations: 0.5% for $^{87}Rb/^{86}Sr$, 0.5% for $^{147}Sm/^{144}Nd$, 0.03% for $^{87}Sr/^{86}Sr$, and 0.005% for $^{143}Nd/^{144}Nd$. The ε_{Nd} was determined accurate to ±0.5, which corresponds to the precision of Rb–Sr and Sm–Nd analyses at the Institute of Precambrian Geology and Geochronology, Russian Academy of Sciences.

The samples of basalts selected for U–Pb isotopic analysis were preliminarily washed in a very weak HCl solution to remove surface pollutants. Some samples were subsequently leached in concentrated HNO_3 and HCl at 90°C. The leached and unleached samples were decomposed in a mixture of concentrated HNO_3 and HF.

The Pb isotopic composition and Pb and U contents were determined in aliquots using a mixed ^{235}U-^{208}Pb spike. U and Pb were extracted using the Mane method. The isotopic composition of U and Pb was measured on a Finnigan MAT-261 multicollector mass spectrometer

Table 2. Sm–Nd data on rocks and minerals

No.	Sample	Sm (ppm)	Nd (ppm)	$^{147}Sm/^{144}Nd$	$^{143}Nd/^{144}Nd$	K_2O (wt %)	P_2O_5 (wt %)	$\varepsilon_{Nd}(120)$
1	2134-1 whole rock	3.622	12.71	0.1707	0.512806 ± 20	0.45	0.15	3.7
2	2134-1 plagioclase	0.2088	0.990	0.1269	0.512766 ± 36	–	–	–
3	2134-1 pyroxene	1.896	4.790	0.2371	0.512900 ± 16	–	–	–
4	2335-1 whole rock	3.423	12.10	0.1694	0.512905 ± 16	0.28	0.13	5.6
5	2335-1 plagioclase	0.1117	0.550	0.1222	0.512823 ± 116	–	–	–
6	2335-1 pyroxene	1.540	3.750	0.2462	0.512944 ± 11	–	–	–
7	2354-1 whole rock	6.787	26.23	0.1550	0.512904 ± 9	0.60	0.35	5.8
8	2354-1 plagioclase	0.3773	1.760	0.1283	0.512786 ± 31	–	–	–
9	2354-1 pyroxene	6.619	25.79	0.1537	0.512899 ± 13	–	–	–
10	2359-1a whole rock	8.367	35.68	0.1405	0.512864 ± 10	0.73	0.35	5.3
11	2359-1a plagioclase	0.5190	2.690	0.1154	0.512798 ± 41	–	–	–
12	2359-1a pyroxene	3.914	10.99	0.2133	0.512925 ± 9	–	–	–
13	3068-r whole rock	2.902	10.14	0.1730	0.512927 ± 18	0.27	0.19	6.0
14	3068-r plagioclase	0.113	0.519	0.1318	0.512855 ± 20	–	–	–
15	3068-r pyroxene	2.993	9.408	0.1923	0.512942 ± 14	–	–	–
16	3674-1 whole rock	7.641	31.47	0.1467	0.512669 ± 7	1.10	0.32	1.4
17	3674-1 plagioclase	0.700	3.456	0.1223	0.512581 ± 35	–	–	–
18	3674-1 pyroxene	3.645	10.74	0.2050	0.512698 ± 12	–	–	–
19	3054 whole rock	7.671	31.55	0.1469	0.512662 ± 5	1.40	0.35	1.2
20	3054 plagioclase	0.848	4.022	0.1274	0.512567 ± 18	–	–	–
21	3054 pyroxene	3.988	13.66	0.1765	0.512657 ± 16	–	–	–
22	3654-5 whole rock	7.524	29.01	0.1569	0.512839 ± 11	0.49	0.31	4.6
23	3654-5 plagioclase	0.255	1.273	0.1209	0.512749 ± 16	–	–	–
24	3654-5 pyroxene	2.868	7.588	0.2284	0.512909 ± 15	–	–	–
25	3672-f whole rock	7.880	30.34	0.1570	0.512864 ± 15	0.91	0.30	5.0
26	3672-f plagioclase	0.176	0.982	0.1081	0.512473 ± 21	–	–	–
27	3672-f pyroxene	2.664	6.748	0.2385	0.512879 ± 14	–	–	–
28*	3069-b whole rock	3.81	13.37	0.1722	0.512864 ± 9	0.22	0.18	4.8
29*	3069-b plagioclase	0.103	0.488	0.1282	0.512854 ± 55	–	–	–
30*	3069-b pyroxene	1.81	4.37	0.2499	0.512927 ± 50	–	–	–
31*	3072 whole rock	11.33	48.63	0.1409	0.512828 ± 10	1.52	0.50	4.6
32*	3072 plagioclase	0.376	2.11	0.1076	0.512827 ± 19	–	–	–
33*	3072 pyroxene	4.46	12.51	0.2155	0.512916 ± 14	–	–	–
34	5505/1a whole rock	4.270	14.62	0.1765	0.512966 ± 15	0.19	0.18	6.7
35	5505/1a plagioclase	0.197	0.856	0.1393	0.512927 ± 24	–	–	–
36	5505/1a pyroxene	3.944	12.20	0.1953	0.512954 ± 11	–	–	–
37	5542-2 whole rock	8.140	33.40	0.1460	0.512608 ± 8	1.27	0.30	0.2
38*	3652-2a whole rock	7.79	30.34	0.1552	0.512770 ± 10	1.02	0.30	3.2

Note: Measurements were performed in Kanzas University (analyst N.R. van Schmus).

Table 3. Rb–Sr data on rocks and minerals

No.	Sample	Rb (ppm)	Sr (ppm)	$^{87}Rb/^{86}Sr$	$^{87}Sr/^{86}Sr$	$(^{87}Sr/^{86}Sr)_0$
1	5505/1a rock	2.201	189.0	0.0337	0.704312 ± 45	0.704255 ± 45
2	5505/1a plagioclase	0.519	338.3	0.0044	0.704183 ± 26	–
3	2134-1 rock	12.00	197.8	0.1755	0.705420 ± 26	0.705121 ± 26
4	2134-1 plagioclase	7.941	292.1	0.0785	0.705107 ± 5	–
5	2335-1 rock	10.58	191.8	0.1596	0.705055 ± 14	0.704783 ± 14
6	2335-1 plagioclase	1.955	312.0	0.0181	0.704886 ± 15	–
7	2359/1a rock	21.83	514.3	0.1228	0.705422 ± 11	0.705213 ± 11
8	2354-1 rock	18.11	327.6	0.1599	0.704596 ± 12	0.704323 ± 12
9	2354-1 plagioclase	1.724	625.3	0.0080	0.704513 ± 46	–
10	2361-3 rock	16.94	427.0	0.1148	0.704494 ± 14	0.704298 ± 14
11	2819-2 rock	2.053	197.7	0.0300	0.704742 ± 72	0.704691 ± 72
12	2819-2 plagioclase	0.765	293.1	0.0075	0.704281 ± 18	–
13	2840-2 rock	5.984	199.8	0.0866	0.704975 ± 32	0.704823 ± 32
14	2840-2 plagioclase	0.563	325.0	0.0050	0.705069 ± 13	–
15	2827-3 rock	14.46	396.1	0.1056	0.704899 ± 85	0.704719 ± 85
16	2827-3 plagioclase	1.776	699.6	0.0073	0.704179 ± 27	–

Note: $(^{87}Sr/^{86}Sr)_0$ is calculated for 120 Ma.

in a mode of the simultaneous record of the ion currents of all isotopes. The measured Pb ratios were corrected for a fractionation coefficient of 0.13% per mass unit, which was determined by the replicate measurements of the Pb isotope composition in the NBS SRM-982 standard. The laboratory blank was 0.4 ng for Pb and

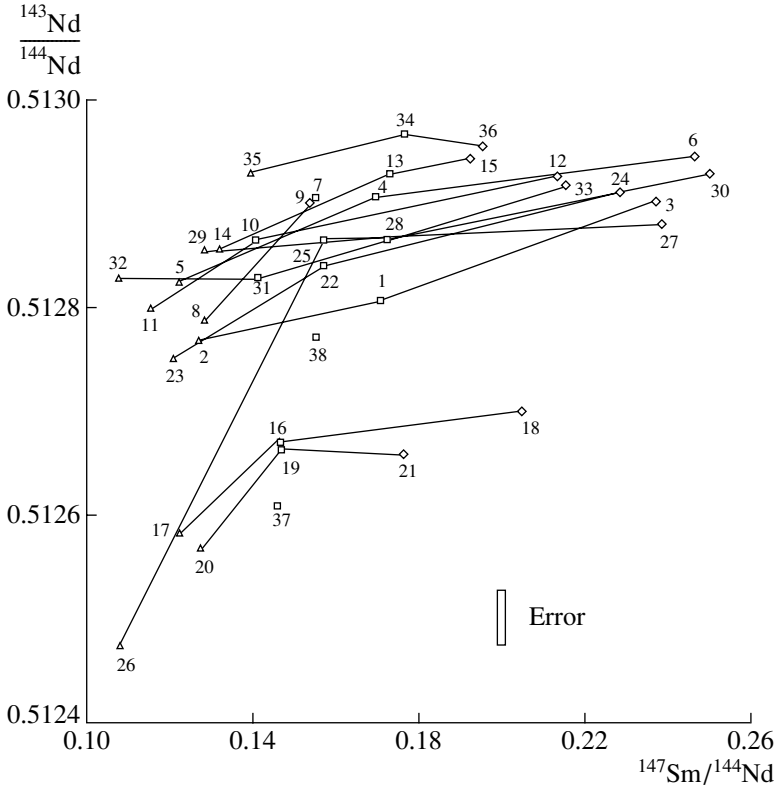

Fig. 2. Correlation of $^{143}Nd/^{144}Nd$ with $^{147}Sm/^{144}Nd$. Box is the whole-rock; diamond is pyroxene; triangle is plagioclase. Numbers correspond to those in Table 2.

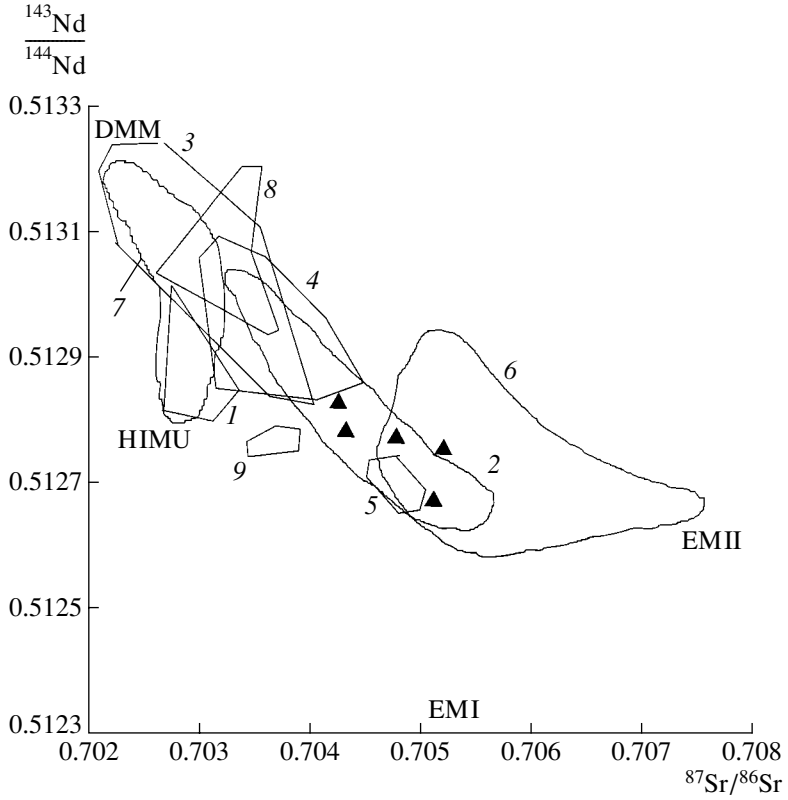

Fig. 3. Correlation of $^{143}Nd/^{144}Nd$ with $^{87}Sr/^{86}Sr$. Triangles denote FJL basalts. Mantle domains, islands, and archipelagos: (*1*) St. Helena, (*2*) Azores, (*3*) MORB, (*4*) Hawaii, (*5*) Kerguelen, (*6*) Samoa, (*7*) Madeira, (*8*) Iceland, (*9*) Trinidad (hereinafter data from [1–13]).

0.05 ng for U. The measured data was processed with the PBDAT program.

RESULTS

The results obtained by measuring the Sr, Nd, and Pb isotopic composition and the contents of Rb, Sr, Sm, Nd, U, Pb in whole rocks and minerals are presented in Tables 1–3 and Figs. 2–6. As can be seen from these data, the Sm and Nd contents in the rock are not balanced by those in minerals (*Pl*, *Px*) for most samples (samples 3068C, 5505/1a, and others). The unbalance is insignificant only in some samples (3674-1, 3054, and others). A similar disagreement is observed for the Rb–Sr system. The Sr contents in whole-rock samples are presumably completely accounted for by plagioclase, but the Rb content is in excess.

The subalkali basalts have almost zero values of ε_{Sr}, moderately positive ε_{Nd}, and relatively high ratios of $^{206}Pb/^{204}Pb$, $^{207}Pb/^{204}Pb$, and $^{208}Pb/^{204}Pb$. The tholeiites exhibit positive values of ε_{Sr} and ε_{Nd} and a less radiogenic Pb isotopic composition. The most radiogenic Pb was found in the subalkali basalt 5542/2, while the tholeiite basalts 5505a bears less radiogenic Pb.

DISCUSSION

Isotopic–geochronologic investigations of rocks and minerals. The isotopic ages of both continental and island basalts is difficult to determine, primarily because of the absence of minerals suitable for dating. The K–Ar dates range widely, from 52, 74, 92, 125, 133 Ma for whole-rock samples to 316, 327, and 555 Ma for plagioclases, at the aforementioned stratigraphic age of 120–140 Ma [18]. The whole-rock ages were disturbed mainly owing to the partial loss of radiogenic Ar during weathering of matrix glasses, the main concentrators of K and radiogenic Ar. Plagioclase typically contains excess Ar (entrapped or inherited), which causes overestimated ages.

The presence of minerals or, presumably, individual phases in minerals with relatively high Rb/Sr ratios are required to obtain reliable age estimates [19]. Reliable dates can be obtained even at a relatively low $^{87}Rb/^{86}Sr$ ratio, such as that in the FJL basalts (≤0.17), if one of the measured components with an extremely low Rb/Sr ratio (plagioclase in our rocks) provides a reliable initial $(^{87}Sr/^{86}Sr)_i$ ratio. However, as can be seen from Table 3, this ratio exhibits wide variations, yielding a wide scatter in dates from 80 Ma for sample 2840-2 to 1429 Ma for sample 2819-2. Samples 2134-1, 2335-1, and 2354-1, which have similar $(^{87}Sr/^{86}Sr)_i$ ratios of

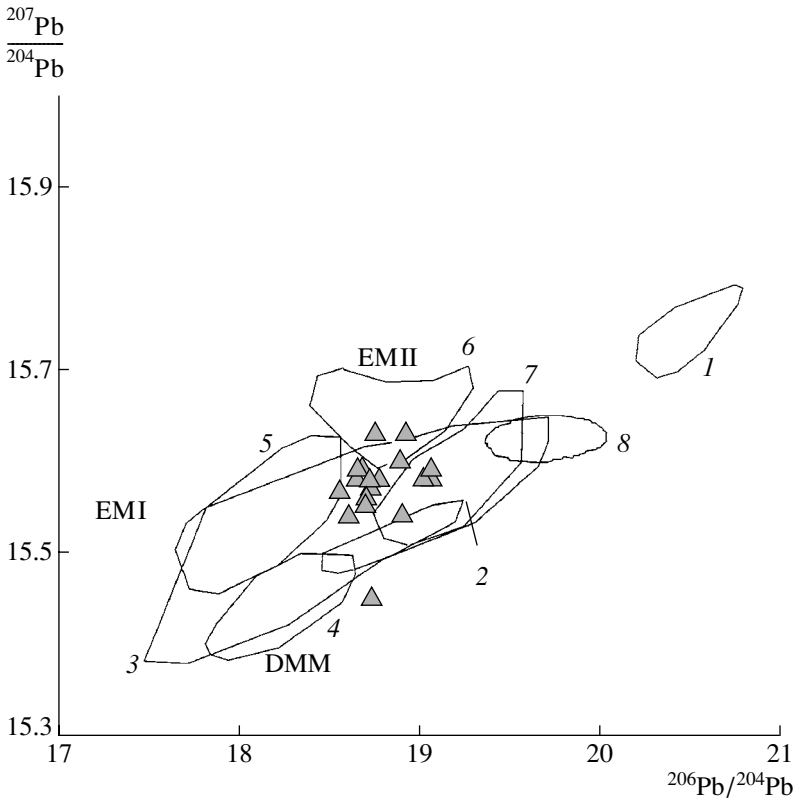

Fig. 4. Correlation of $^{207}Pb/^{204}Pb$ with $^{206}Pb/^{204}Pb$. Triangles are basalts of FJL. (*1*) St. Helena, (*2*) Iceland, (*3*) MORB, (*4*) Hawaii, (*5*) Kerguelen, (*6*) Samoa, (*7*) Madeira, (*8*) Azores.

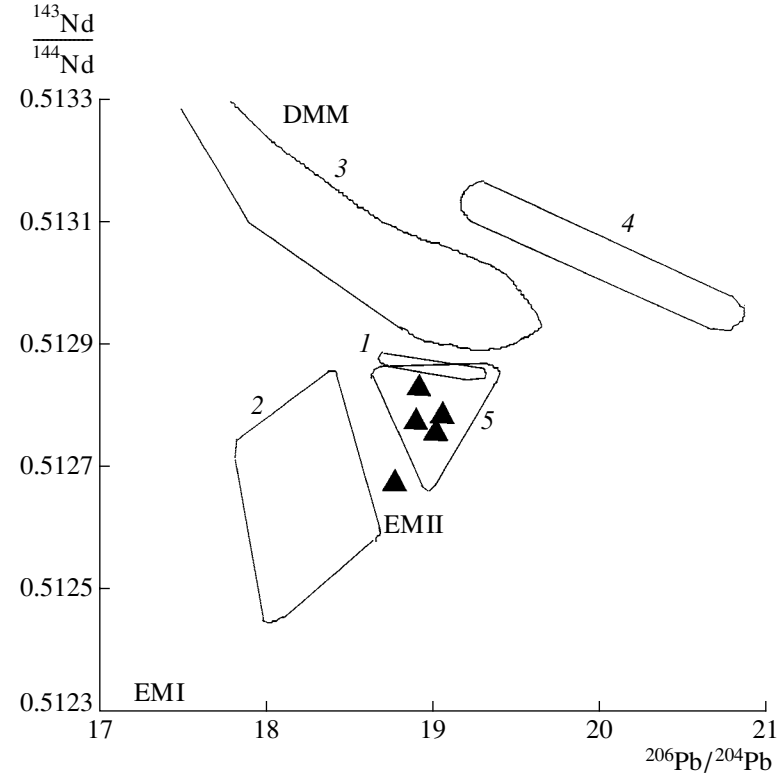

Fig. 5. Correlation of $^{143}Nd/^{144}Nd$ with $^{206}Pb/^{204}Pb$. Triangles are basalts of FJL. (*1*) Amsterdam, St. Paul, (*2*) Kerguelen, (*3*) MORB, (*4*) St. Helena, (*5*) kimberlites (gr. II).

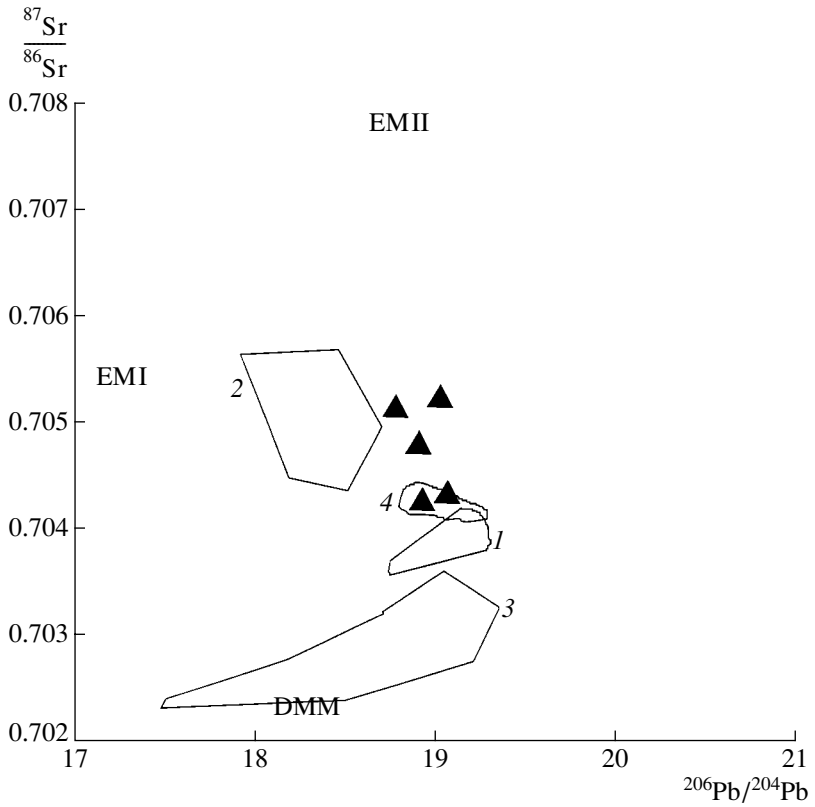

Fig. 6. Correlation of $^{87}Sr/^{86}Sr$ with $^{206}Pb/^{204}Pb$. Triangles are basalts of FJL. (*1*) Amsterdam, St. Paul, (*2*) Kerguelen, (*3*) MORB, (*4*) Croiset.

0.70485 ± 27, 0.70486 ± 16, and 0.70451 ± 15, define an age close to the stratigraphic one, although with a large error.

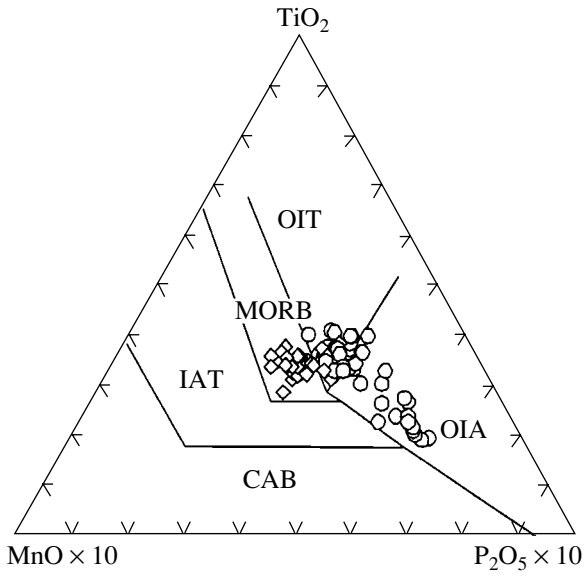

Fig. 7. Discriminant diagram $Mn–TiO_2–P_2O_5$ for flood-basalt complex of FJL; diamonds are tholeiitic basalts, circles are subalkaline basalts; fields: (CAB) calc-alkaline basalts; (IAT) island arc tholeiites; (MORB) mid-ocean ridge basalts; (OIT) oceanic island tholeiites; (OIA) ocean island andesites.

Unexpected results were obtained for the Sm–Nd systems (Table 2, Fig. 2). In spite of the relatively large error, some samples yield nearly stratigraphic isochron ages (on plagioclase, whole-rock, and pyroxene) but display distinct evidence for isotopic disequilibrium. Thus, the age scatter has geochemical reasons (which will be discussed below) and is not caused by analytical errors. However, in any event, the use of isotopic geochronology at this stage does not define the age relations between the tholeiitic and subalkali basalts.

Position of FJL in the Global Sr–Nd–Pb Systematics

It is seen in Figs. 3–6 that the basaltic rocks of the FJL are plotted within the fields of other islands, including archipelagos [1–15], which is consistent with the concepts of the common origin of island basalts. The Sm, Nd, and Pb isotopic composition moderately varies for different samples, which is also more or less typical of other islands. However, as is seen from the correlation isotopic curves, the data points are displaced from the depleted to the enriched reservoir EM II [20]. This reservoir is referred to as a local long-term reservoir enriched in incompatible elements, or, more probably, as that derived from crust and/or sediments (mainly, terrigenous). It should be noted that some data [21–26], including those of FJL, point to a significant,

if not predominant, role of mixing between the depleted and enriched reservoirs. This casts some doubts, which are beyond the scope of our paper, on the recognition of the OIB source of island basalts as a uniform and long-term mantle enclave. Similarly, continental basalts can also be produced by the mixing of depleted and enriched components [27–34].

The absence of crustal (sedimentary) contamination is hardly possible. The extent of magma interaction with the relatively cold walls of the channel during its ascent depends on many parameters, such as the magma temperature, the rate of its movement (the maximum assimilation is attained at optimum value ~2000 Reynold's numbers [35]), the specific area of the intrusion, and the presence of a fluid phase. The measured effect of interaction between the chamber walls and magma is finally defined by differences in the isotopic and chemical composition, including major elements, which allow discrimination between the tholeiite and subalkali basalts of FJL (Fig. 7).

Most previous isotopic investigations, which were performed mainly with whole-rock samples, reveal a mixing effect. However, the use of individual minerals in addition to whole rock samples is required for more detailed analysis.

Estimate of Contamination Effect on the Isotopic Equilibrium

As was mentioned above, an at least two-component mixture of depleted and enriched material is required to explain the data obtained on island and continental basalts. However, physicochemical processes defining mixing remain unclear. In particular, it should be determined in what form the contamination occurred. The mixing of magmas of similar major-element compositions is shown in Fig. 8a. Sample A is higher in enriched component *P*2. If the isotopic system was not disturbed after crystallization, two mineral isochrons (in the general case, *n* isochrons) with different initial $^{143}Nd/^{144}Nd$ ratios define the time of termination of crystallization and the closure of the isotopic systems. The line connecting points *P*1, *WR*(A), *WR*(B), and *P*2 is the mixing line and has no age sense. However, Fig. 8a is not consistent with the experimental data shown in Fig. 2. It can be hypothesized that the contamination of the depleted (~mantle) component did not affect the mineral, i.e., influenced only on the matrix (~glass) (Fig. 8b), but this is, again, inconsistent with most data in Fig. 2. Evidently, the matrix and minerals were contaminated differently, i.e., $P1/P2(WR) \neq P1/P2(Px) \neq P1/P2(P1)$. One of the possible variants is the chaotic mixing of the whole rock and minerals of samples A and B in the laboratory (Fig. 8c). This situation seems to be hardly probable, and the following scenario can be more realistic. During the crystallization of the initial (depleted) material, material from reservoir *P*2 enriched in incompatible elements was accommodated in both the whole rocks and the minerals (Fig. 8d). The mixing must have occurred when crystallization began and individual minerals formed but before the end of this process. Otherwise, enriched material should have been completely accumulated in the matrix glass, i.e., a situation analogous to that in Fig. 8b. It should be noted that none of the scenarios considered above can be described by the model of assimilation and fractional crystallization in its pure form [36–39].

Assimilation and enrichment caused by the CO_2–phosphate fluid, the most abundant metasomatic agent, can trigger the chemical differentiation of the initial silicate phase and metasomatic carbonates and phosphates, and this should eventually lead to the straightening of the polygonal line (Fig. 2) and the obtaining of isochron dependences having an age sense. The data in

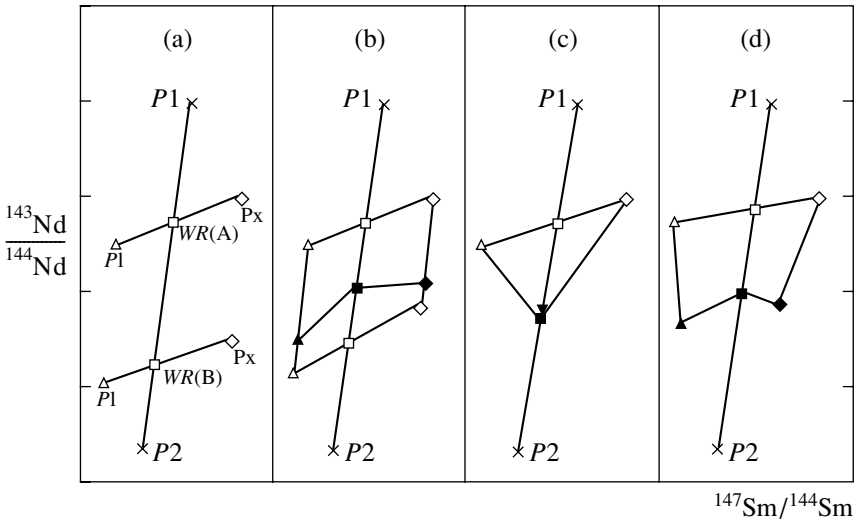

Fig. 8. Scheme of mixing of two reservoirs, *P*1 (depleted) and *P*2 (enriched). Filled symbols are the mixing result (see text for explanation).

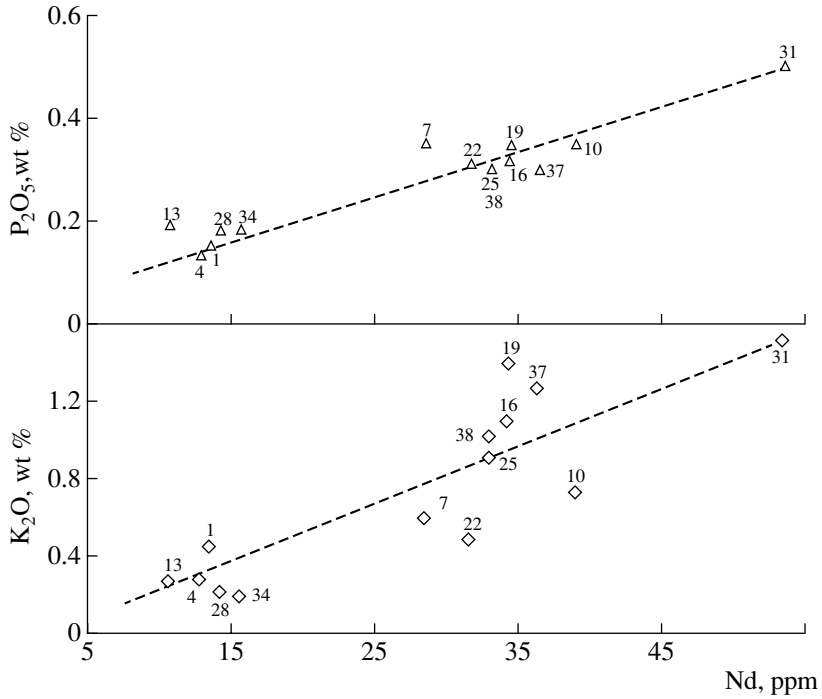

Fig. 9. Correlation of P_2O_5 and K_2O with Nd content.

Fig. 9 definitely demonstrate a correlation between incompatible elements in the inferred metasomatic component [40, 41].

CONCLUSIONS

Isotopic–geochemical data on islands of the Franz Josef Land Archipelago are plotted in the isotopic field of oceanic islands. Thus, the OIB reservoir of the Arctic Ocean is close or similar to the corresponding sources of islands of the Pacific, Indian, and Atlantic oceans.

The primary tholeiitic magma was enriched in material from the mantle domain EII (crust and sedimentary cover). The chemical and isotopic composition of the subalkali basalts (basaltic andesites) corresponds to this scenario. The carrier of incompatible elements, including Nd with a low $^{143}Nd/^{144}Nd$ ratio and Sr with a high $^{87}Sr/^{86}Sr$ ratio, was a metasomatic fluid with crustal chemical and isotopic signatures. This fluid caused the disequilibrium detected in the isotopic systems, in particular, the disturbance of the Sm–Nd mineral isochrons.

ACKNOWLEDGMENTS

This study was supported by the Russian Foundation for Basic Research (project no. 03–05-64779) and Program no. 7 of the Department of Earth Sciences of Russian Academy of Sciences.

REFERENCES

1. M. Tatsumoto, "Isotopic Composition of Lead in Volcanic Rocks from Hawaii, Two Jima, and Japan," Geophys. Res. **71**, 1721–1733 (1966).
2. S. S. Sun and G. N. Hanson, "Evolution of the Mantle: Geochemical Evidence from Alkali Basalt," Geology **3**, 297–302 (1975).
3. W. M. White, "Sources of Oceanic Basalts: Radiogenic Isotope Evidence," Geology **13**, 115–118 (1985).
4. S. R. Hart, "Heterogeneous Mantle Domains: Signatures, Genesis and Mixing Chronologies," Earth Planet. Sci. Lett. **90**, 273–276 (1988).
5. J. D. Woodhead and M. T. McCulloch, "Ancient Seafloor Signals in Pitcairn Island Lavas and Evidence for Large Amplitude, Small Length-Scale Mantle Heterogeneities," Earth Planet. Sci. Lett. **94**, 257–273 (1989).
6. B. Dupre, B. Lambert, and C. J. Allegre, "Isotopic Variations within a Single Oceanic Island: The Terceira Case," Nature **299**, 620–622 (1982).
7. R. V. Fodor and B. B. Hanan, "Geochemical Evidence for the Trinidade Hotspot Trace: Columbia Seamount Ankaramite," Lithos **51**, 293–304 (2000).
8. D. C. Gerlach, R. A. Cliff, G. R. Davies, et al., "Magma Sources of the Cape Verde Archipelago: Isotopic and Trace Element Constraints," Geochim. Cosmochim. Acta **52**, 2970–2992 (1988).
9. Y. Nakamura and M. Tatsumoto, "Pb, Nd and Sr Isotopic Evidence for a Multicomponent Source for Rocks of the Cook-Austral Islands and Heterogeneities of Mantle Plumes," Geochim. Cosmochim. Acta **52**, 2909–2924 (1988).
10. J. Mata, R. Kerrich, N. D. MacRae, and T.-W. Wu, "Elemental and Isotopic (Sr, Nd and Pb) Characteristics of

Madeira Island Basalts: Evidence for a Composite HIMU-EMI Plume Fertilizing Lithosphere," Can. J. Earth Sci. **35**, 980–997 (1998).

11. L. N. Kogarko, L. K. Levskii, and N. F. Gushchina, "Isotope Sources of Hot Spots in the Trindade and Martin Vaz Islands, Southwestern Atlantic," Dokl. Akad. Nauk **392**, 678–681 (2003) [Dokl. Earth. Sci. **392**, 1116 (2003)].
12. R. Doucelance, S. Escrig, M. Moreira, et al., "Pb–Sr–He Isotopic and Trace Element Geochemistry of the Cape Verde Archipelago," Geochim. et Cosmochim. Acta **67**, 3717–3733 (2003).
13. B. Kieffer, N. T. Arndt, and D. Weis, "A Bimodal Alkalic Shield Volcano on Skiff Bank: Its Place in the Evolution of the Kerguelen Plateau," J. Petrol. **43**, 1254–1286 (2002).
14. H. Amundsen, A. Evdokimov, V. D. Dibner et al., "The Northern Barents Sea Geotraverse," Norsk Polarinstitutt Meddelelser, No. 151, 105–120 (1998).
15. T. Ntaflos and W. Richter, "Geochemical Constraints on the Origin of the Continental Flood Basalt Magmatism in Franz Josef Land, Arctic Russia," Eur. J. Mineral. **15**, 649–663 (2003).
16. E. A. Chernysheva, G. S. Kharin, and N. M. Stolbov, "Basalts from the Franz Josef Land Archipelago: New Geochemical Data," Dokl. Akad. Nauk **390**, 258–261 (2003) [Dokl. Earth Sci. **390**, 550 (2003)].
17. A. N. Evdokimov and N. M. Stolbov, "Basic Rocks of Franz Josef Land: Chemical Character and Geodynamic Setting," in *Proceedings of Fourth Intern. Conf. Arctic Margins-ICAM IV. Dartmouth. Nova Scotia, Canada* (Dartmouth, 2003), pp. 44–45.
18. N. M. Stolbov, "On the Problem of the Age of Flood-Basalt Magmatism of the Franz Josef Land Archipelago on the Basis of Radiological Data," in *Geological–Geophysical Characteristics of Lithosphere of the Arctic Region* (2002), vol. 4, pp. 199–202.
19. S. Ingle, D. Weis, and F. A. Frey, "Indian Continental Crust Recovered from Elan Bank Kerguelen Plateau (ODP Leg183, Site1137)," J. Petrol. **43**, 1241–1257 (2002).
20. A. Zindler and S. Hart, "Chemical Geodynamics," Ann. Rev. Earth Plan. Sci. **14**, 493–571 (1986).
21. Z. A. Palacz and A. D. Saunders, "Coupled Trace Element and Isotope Enrichment in the Cook-Austral-Samoa Islands, Southwest Pacific," Earth Planet. Sci. Lett. **79**, 270–280 (1986).
22. J. Barling, S. L. Goldstein, and I. A. Nickolls, "Geochemistry of Heard Island (Southern Indian Ocean): Characterization of An Enriched Mantle Component and Implications for Enrichment of the Sub-Indian Ocean Mantle," J. Petrol. **35**, 1017–1053 (1994).
23. C. R. Neal, J. J. Mahoney, and W. J. Chazey III, "Mantle Sources and the Highly Variable Role of Continental Lithosphere in Basalt Petrogenesis of the Kerguelen Plateau and Broken Ridge LIP: Results from ODP Leg 183," J. Petrol. **43**, 1177–1205 (2002).
24. J. C. Lassiter, D. J. De Paolo, and J. J. Mahoney, "Geochemistry of the Wrangellia Flood Basalt Province: Implications for the Role of Continental and Oceanic Lithosphere in Flood Basalt Genesis," J. Petrol. **36**, 983–1009 (1995).
25. A. E. Saal, S. R. Hart, N. Shimizu, et al., "Pb Isotope Variability in Melt Inclusions from Oceanic Island Basalts, Polynesia," Science **282**, 1481–1484 (1998).
26. F. A. Frey, D. Weis, A. Borisova, and G. Xu, "Involvement of Continental Crust in the Formation of the Cretaceous Kerguelen Plateau: New Perspectives from ODP Leg 120 Sites," J. Petrol. **43**, 1207–1239 (2002).
27. R. R. Doe, P. W. Lipman, C. E. Hedge, et al., "Primitive and Continental Basalts from the Southern Rocky Mountains, USA," Contrib. Mineral. Petrol. **21**, 142–146 (1969).
28. R. W. Carlson, G. W. Lugmair, and J. D. MacDougal, "Columbia River Volcanism: the Question of Mantle Heterogeneity or Crustal Contamination," Geochim. Cosmochim. Acta **45**, 2483–2499 (1981).
29. A. F. Glazner and G. L. Farmer, "Production of Isotopic Variability in Continental Basalts by Cryptic Crustal Contamination," Science **255**, 72–74 (1991).
30. J. D. Landoll, K. A. Foland, and C. M. B. Henderson, "Nd Isotopes Demonstrate the Role of Contamination in the Formation of Coexisting Quartz and Nepheline Syenites at the Abu Khrug Complex, Egypt," Contrib. Mineral. Petrol. **117**, 305–329 (1994).
31. M. T. McCulloch, T. K. Kyser, J. D. Woodhead, et al., "Pb–Sr–Nd–O Isotopic Constraints on the Origin of Rhyolites from the Taupo Volcanic Zone of New Zealand: Evidence for Assimilation Followed by Fractionation from Basalt," Contrib. Mineral. Petrol. **115**, 303–312 (1994).
32. A. Simonetti and K. Bell, "Nd, Pb and Sr Isotopic Data from the Napak Carbonatite–Nephelinite Central Eastern Uganda: An Example of Open-System Crystal Fractionation," Contrib. Mineral. Petrol. **115**, 356–366 (1994).
33. J. F. Luhr, J. G. Pier, J. J. Aranda-Gomez, and F. A. Podosek, "Crustal Contamination in Early Basin and Range Hawaiites of the Los Encinos Field, Central Mexico," Contrib. Mineral. Petrol. **118**, 321–339 (1995).
34. S. A. Prevec, "Sm–Nd Isotopic Evidence for Crustal Contamination in the ca. 1750 Ma Wanapitei Complex, Western Grenville Province, Ontario," Can. J. Earth Sci. **32**, 486–495 (1995).
35. H. E. Huppert and R. S. Sparks, "Cooling and Contamination of Mafic and Ultramafic Magmas During Ascent Through Continental Crust," Earth Planet. Sci. Lett. **74**, 371–386 (1985).
36. H. P. J. Tilton, "The Effects of Assimilation of Country Rocks by Magmas on $^{18}O/^{16}O$ and $^{87}Sr/^{86}Sr$ Systematics in Igneous Rocks," Earth Planet. Sci. Lett. **47**, 243–254 (1980).
37. D. J. De Paolo, "Trace Element and Wallrock Assimilation and Fractional Crystallization," Earth Planet. Sci. Lett. **53**, 189–202 (1981).
38. I. H. Campbell and J. S. Turner, "A Laboratory Investigation of Assimilation at the Top of a Basaltic Magma Chamber," J. Geol. **95**, 155–172 (1987).
39. E. B. Watson, "Basalt Contamination of Continental Crust: Some Experiments and Models," Contrib. Mineral. Petrol. **80**, 73–87 (1982).
40. W. M. White, "Source of Oceanic Basalts: Radiogenic Isotope Evidence," Geology **13**, 115–118 (1985).
41. E. S. Bogomolov and L. K. Levskii, "Sm–Nd and Rb–Sr Isotopic Systematics of Rocks during Metasomatism," Geokhimiya, No. 5, 467–475 (2002) [Geochem. Int., No. 5, 417 (2002)].